2019

A stochastic air combat logistics decision model for Blue versus Red opposition

Seagren, Chad W.; Gaver, Donald P.; Jacobs, Patricia A.

Wiley

Seagren, Chad W., Donald P. Gaver, and Patricia A. Jacobs. "A stochastic air combat logistics decision model for Blue versus Red opposition."Naval Research Logistics (NRL)66.8 (2019): 663-674.

http://hdl.handle.net/10945/65673

Received: 14 September 2018 | Revised: 27 September 2019 | Accepted: 4 October 2019 | Published on: 6 November 2019

DOI: 10.1002/nav.21876

RESEARCH ARTICLE

WILEY

A stochastic air combat logistics decision model for Blue versus Red opposition

Chad W. Seagren[1] | **Donald P. Gaver**[2] | **Patricia A. Jacobs**[2]

[1]Graduate School of Defense Management, Naval Postgraduate School, Monterey, California
[2]Operations Research Department, Naval Postgraduate School, Monterey, California

Correspondence
Chad W. Seagren, Graduate School of Defense Management, Naval Postgraduate School, Monterey, CA.
Email: cwseagre@nps.edu

Abstract

Technologically advanced aircraft rely on robust and responsive logistics systems to ensure a high state of operational readiness. This paper fills a critical gap in the literature for combat models by closely relating effectiveness of the logistics system to determinants of success in combat. We present a stochastic diffusion model of an aerial battle between Blue and Red forces. The number of aircraft of Blue forces aloft and ready to be aloft on combat missions is limited by the maximum number of assigned aircraft, the reliability of aircraft subsystems, and the logistic system's ability to repair and replenish those subsystems. Our parsimonious model can illustrate important trade-offs between logistics decision variables and operational success.

KEYWORDS

air combat, diffusion model, logistics

1 | MODELS OF LOGISTICS AND COMBAT

Technologically advanced and specialized aircraft must rely on robust and responsive logistics systems to ensure that the aircraft are maintained in a high state of readiness. An aircraft maintained to a sufficient level so as to be ready to employ on a combat mission is a necessary component of operational success. Yet, despite the clear importance of logistics effectiveness to operational success, few combat models include relevant aspects of these systems. This paper helps to fill a critical gap in the literature for combat models by closely relating logistics systems' performances to determinants of success in combat.

In this paper, we present a model of aerial combat. We take the classical model of Lanchesterian air combat that consists of a system of ordinary differential equations as a point of departure (Lanchester, 1916). Our model can accommodate a wide variety of operational considerations, such as air-to-air engagements and a variety of different operational parameters like lethality and endurance. In addition, it can accommodate the mechanical reliability of multiple subsystems and the corresponding performance of the logistics system with respect to resupply and repair of those subsystems. The model can relate a variety of operational and support parameters to the probability of operational success.

While we focus on unmanned aircraft in this paper, our model easily accommodates manned aircraft as well. Despite, or perhaps because of, the technological advancement of unmanned aircraft, they still require a high level of maintenance and logistical attention. Our model is intended for a variety of uses. Our model can be employed to study the effects of a new platform design or existing platform modification and the resulting logistic requirements on the probability of mission success; and to explore trade-offs between operational design characteristics and logistics characteristics, as they relate to probability of mission success. In addition, our model can be used at an operational level to examine the operational effects of various decisions such as where to employ aircraft and how to arrange logistics support.

Finally, an important innovation of our model is the inclusion of a stochastic diffusion process that enables the model to provide a distribution of outcomes; cf. Arnold (1974) and Øksendal (2013). The diffusion model represents interrelated dynamics; see Perlas and Lehoczky (1977) for related work. Other related works appear in Bracken, Kress, and Rosenthal (1995), and more recently in Washburn and Kress (2009). The

diffusion model allows assessment of the nonlinear effect of Red and Blue logistics on the outcomes of air combat and the effect of uncertainty on measures of performance. Quantifying this uncertainty enables the model to provide valuable insight into the risk associated with various courses of action.

The approach we employ in this paper holds several advantages over alternative methods, such as simulation modeling. The diffusion model is parsimonious with transparent assumptions. The equations can be modified to represent other assumptions to examine their effects. In addition, the study and display of the time evolution of measures of performance are arguably easier with the diffusion model.

Our paper contributes to three streams of literature. First, it includes a deterministic model of air combat and thus extends that long literature. Second and most important, it helps to fill a critical gap by emphasizing logistics considerations and can relate such considerations to probability of operational success. Finally, it contributes to the stream of literature on applications of stochastic diffusion models. Such an application provides invaluable information regarding the dynamic relationship between the parameters and the measures of performance.

Section 2 of the paper describes the diffusion model in terms of a system of stochastic differential equations. The diffusion model is a Markov process. Section 2 also discusses a limiting model for many aircraft on both sides. Section 3 presents results comparing limiting model means and standard deviations with those from a simulation of a related continuous-time Markov chain with 30 aircraft on each side. The example in Section 4 uses the limiting model to illustrate the importance of the logistics system to operational success in a given scenario.

1.1 | A review of the literature

Aerial warfare was one of the first areas to draw the attention of analysts seeking to improve a military force's chances of success. Lanchester's (1916) seminal work continues to inspire a rich and varied literature that includes analyses of combat on the ground (Bonder, 1967; Taylor, 1983), at sea (Hughes, 1995), in the air (Gilbert, 2011; McLemore, Gaver, & Jacobs, 2016), and in more general terms (Brackney, 1959). Researchers have extended the original deterministic model to include stochastic varieties (Ancker, 1967; Karr, 1974; Kress & Talmor, 1999) and have developed simulation models with Lanchestarian qualities (eg, Artelli and Deckro (2008) as well the US Army and Marine Corps' Combat XXI leverage Lanchester [Balogh & Harless, 2003]). Still others have extended such models to consider counterinsurgency (Saie & Ahner, 2018), guerilla warfare (Deitchman, 1962; Schaffer, 1968), and cyberwarfare (Schramm & Gaver, 2013). In addition, researchers have applied Lanchester models to empirical data from actual battles involving humans (Bracken, 1995; Lucas & Turkes, 2004; Weiss, 1966), as well as chimpanzees (Wilson, Britton, & Franks, 2002), and ants (McGlynn, 2000), among others.

A common theme among these combat models is to neglect, or at least minimize, the importance of logistics concerns. Similarly, models of combat logistics systems often omit or have limited views of operational aspects of the combat units that such systems support. One technique is to relate logistics effectiveness to operational "readiness". Kang, Doerr, and Sanchez (2006) develop a model that relates logistical effectiveness to the availability of materiel required by a unit of unmanned aerial vehicles (UAVs). Likewise, Hoover, Jondrow, Trost, and Ye (2002) develop a theoretical model that primarily examines questions at the small unit level relating to performance metrics like aircraft readiness levels resulting from removing working parts from one aircraft to put into another whose parts have failed; see also Gaver, Isaacson, and Abell (1993). Bazin de Jessey and Debache (2002), Kang, Gue, and Eaton (1998), and Kang and McDonald (2010) develop simulation models that relate logistics performance to readiness of deployed aircraft. Similarly, Gue (2003) presents a model to support dispersed operational units supported from the sea, while Huffaker (1996) develops a theater-level model that relates supply throughput to success in combat. In all cases, logistics performance is related to materiel readiness, as opposed to probability of mission success. See Beamon (1998) and Yavuz and Satir (1995) for surveys of the literature on models of supply chain management.

Moglewer and Payne (1970) are an exception to this phenomenon. They model the distribution of supplies throughout the battle-space from a game-theoretic perspective and ultimately relate logistic effectiveness to the probability that the operation is successful. This two-step theater-level game of ground combat is of limited applicability to the case we examine in this paper. Likewise, Chase (1973) is another exception. He employs a Lanchester model of ground combat and includes consideration of logistical capability. Ultimately, he analyzes the choice of how much combat power to devote to protecting supply chains required to sustain the main bodies of the opposing forces.

The literature is sparse for combat models of operational-level air warfare that incorporate the effectiveness of the logistics system as a determinant for success in combat. In this paper, we present a model that fills this critical gap. We model an aerial battle between Blue and Red forces. The number of aircraft that Blue forces can fly on combat missions is limited by the reliability of aircraft subsystems and the logistic system's ability to repair and replenish those subsystems. Our model illustrates several important trade-offs between the number of Blue aircraft, the reliability and maintainability of Red and Blue aircraft, and Blue's ability to successfully complete its mission. This initial study is intended to identify broad effects, and deserves alternative formulations that can be Monte Carlo simulated, and interpreted by expert opinion.

2 | THE MODEL

We envision a situation in which an aircraft unit, Blue (B), engages nearby Red (R) threats in aerial combat. Blue aircraft are supported by facilities and spares in the vicinity, which might include sea-based platforms, amphibious warfare ships, littoral combat ships, or a ground-based system of support. This framework is sufficiently flexible to consider any scale of operation and a wide range of combat intensity. For example, combat intensity could range from a limited strike or show-of-force to sustained and deliberate combat with a near-peer competitor. High-level low-resolution attention is paid to mission readiness degraders, that is, repairable/replaceable subsystems of Blue aircraft.

The model accounts for aircraft in various states of operational readiness. An aircraft can either be aloft (denoted with subscript A), on the ground/tarmac but available (denoted with subscript G), or down due to failure (denoted with subscript C). Both sides' aircraft are launched from available (ready) aircraft on the ground. Each side's launch rate from the ground is proportional to the difference between a user defined maximum desired number of aircraft airborne and the current number airborne. Forces in the air engage each other with aimed fire. Analysis of data suggests that historical air combat may not be well modeled by aimed fire; cf. Johnson and MacKay (2011). However, we assume that future beyond visual range missile combat will increasingly have the characteristics of aimed fire. Under conditions of aimed fire, the number of the opposition aircraft killed increases with the square of the number of aircraft; whereas for un-aimed fire, the relationship between aircraft and number of opposition aircraft killed is linear. This extra weight to numbers of aircraft relative to lethality is at least broadly consistent with certain visions of the importance of numbers of aircraft in the future of air warfare (Clough, 2002). If aimed fire is unsatisfactory, the equations can be modified to include another model. Investigating the effect of differences in these assumptions is the topic of future research.

Aircraft remain airborne until they complete their mission; they are lost to enemy fire; or they experience an operational failure. An operational failure could be a spontaneous loss of operations due to mechanical or electrical failure of some essential subsystem. Aircraft lost to enemy fire cannot be repaired. We defer the study of equations modified to include aircraft damaged by enemy fire and their subsequent repair. Upon returning to base, aircraft with failures must await maintenance action before returning to available status. Returning operational aircraft without failures is available to return to the air after a user-defined turn-around-time. There is a specified maximum total number of aircraft for each side. Both sides' aircraft can be reinforced from outside. Each side's reinforcement rate is proportional to the difference between its user specified maximum total number and current total number.

The time to repair or maintain aircraft is affected by the space available to repair or maintain the aircraft; the number and expertise of personnel; job priorities; the availability of spare parts, and so forth. The time spent waiting for parts often dominates the other factors. The availability of spare parts is affected by the reordering policy, the time to deliver the spare parts, and so forth. For transparency, our model optimistically represents the repair facility as an infinite server queue; that is, all aircraft needing maintenance receive service simultaneously and so will tend to return to ready status sooner than if there is finite repair capability whose model has more parameters. The mean time for delivery of spare parts is incorporated in the mean time to repair. The study of a model representing finite repair capacity and the supply system for delivering spare parts is a subject for future work.

2.1 | Parameters and states

The following parameters are essential for the model and system state variables.

2.1.1 | Planning parameters

$\overline{R}_A$ = maximum Red aircraft aloft;
$\overline{R}$ = maximum total number of Red aircraft; $\overline{R}_A \le \overline{R}$;
$\overline{B}_A$ = maximum Blue aircraft aloft;
$\overline{B}$ = maximum total number of Blue aircraft; $\overline{B}_A \le \overline{B}$.

The quantities $\overline{R}$, $\overline{R}_A$, (respectively $\overline{B}, \overline{B}_A$) are Red (respectively Blue) planning parameters.

2.1.2 | State variables

The following are the state variables described in the differential equations.

- $\boldsymbol{R}_A(t)$, (respectively, $\boldsymbol{B}_A(t)$) = number of Red, (respectively Blue), aircraft aloft at time t.
- $\boldsymbol{R}_G(t)$, (respectively, $\boldsymbol{B}_G(t)$) = number of Red, (respectively Blue), aircraft on the tarmac (ground) ready for operations at time t.
- $\boldsymbol{R}_c(t)$, (respectively, $\boldsymbol{B}_c(t)$) = number of Red, (respectively Blue), aircraft unavailable for operations at time t due to a type c failure, $c = 1, 2, \ldots, C$.
- $\boldsymbol{R}_C(t) = \sum_c \boldsymbol{R}_c(t)$, (respectively, $\boldsymbol{B}_C(t)$) = total number of Red, (respectively, Blue), aircraft unavailable at time t due to failure.

$\{\boldsymbol{W}_\bullet(t); t \ge 0\}$ are independent Gaussian/Wiener processes; $d\boldsymbol{W}_\bullet(t)$ is a Weiner process increment in the interval $(t, t + dt]$; it has a normal distribution with mean 0 and variance dt. In particular, $\{\boldsymbol{W}_{RAK}(t); t \ge 0\}$ is the Weiner process associated with the change in the number of aloft Red aircraft due to attrition; $\{\boldsymbol{W}_{RAR}(t); t \ge 0\}$ is the Weiner process associated with the change in the number of ready Red aircraft on the tarmac due to aloft Red reinforcement; $\{\boldsymbol{W}_{RFc}(t); t \ge 0\}$ is the Weiner

process associated with the change in the number of unavailable Red aircraft due to type c failure; $\{\boldsymbol{W}_{RE}(t); t \geq 0\}$ is the Weiner process associated with the change in the number of aloft Red aircraft due to mission end; $\{\boldsymbol{W}_{RGR}(t); t \geq 0\}$ is the Weiner process associated with the change in the number of Red aircraft due to outside reinforcement; $\{\boldsymbol{W}_{RRc}(t); t \geq 0\}$ is the Weiner process associated with the change in the number of unavailable Red aircraft due to repair completion of a type c failure.

2.1.3 | Rate parameters

The following are the rate parameters that describe behavior of Red and Blue.

- β_R is Red defender aimed fire attrition rate against Blue aloft attackers; an estimate for the parameter is the initial number of Red weapons on an aircraft multiplied by the probability of kill per weapon, the fraction of Red aircraft's mission time Red is in the area of operations (AO), the fraction of Blue aircraft's mission time Blue is in the AO, and divided by the Red aircraft's mission time; β_B is the Blue attacker aimed fire attrition rate against Red.
- α_R is Red (active) aircraft aloft reinforcement rate per fraction of aloft mission capable Red aircraft needed. That fraction is $\left[\frac{\overline{R}_A - \boldsymbol{R}_A(t)}{\overline{R}_A}\right]^+$, where $\overline{R}_A$ is the Red aloft quota and $[\overline{R}_A - \boldsymbol{R}_A(t)]^+$ is Red aloft deficiency, filled from $\boldsymbol{R}_G(t)$. Conventionally, $[x]^+ = \max(x, 0)$. The total reinforcement rate at time t is $\alpha_R\left[\frac{\overline{R}_A - \boldsymbol{R}_A(t)}{\overline{R}_A}\right]^+ \boldsymbol{R}_G(t)$; $1/\alpha_R$ is the mean time to prepare a ready aircraft on the tarmac for flight. This functional form allows the number of Red aircraft aloft to remain less than or equal to the maximum allowed airborne and is proportional to the number of Red aircraft on the tarmac available to fly. Other functional forms are possible; α_B is the Blue (active) aircraft aloft reinforcement rate per fraction of aloft mission capable Blue aircraft needed.
- δ_R is the rate of Red mission termination; while $1/\delta_R$ is the mean mission duration of Red aircraft; δ_B is the rate of Blue mission termination.
- φ_{Rc} is the type c failure rate for an aloft Red aircraft; while $1/\varphi_{Rc}$ is the Red aircraft mean time until type c failure; φ_{Bc} is the type c failure rate for an aloft Blue aircraft.
- μ_{Rc} is the rate at which a failed Red aircraft in need of repair for a type c failure is returned to ready on-tarmac status. Returning an aircraft to a ready status requires maintenance action and may include a wait time for repair parts or replacement subsystem; $1/\mu_{Rc}$ is the mean time to repair a type c failure for a Red aircraft; μ_{Bc} is the rate at which a failed Blue aircraft in need of repair for a type c failure is returned to ready on-tarmac status.
- γ_R is the Red ground reinforcement rate per fraction of aircraft needed, $\left[\frac{\overline{R} - \boldsymbol{R}_A(t) - \boldsymbol{R}_G(t) - \sum_c \boldsymbol{R}_c(t)}{\overline{R}}\right]^+$, with $\overline{R}$ being Red's total defensive quota. Other functional forms are possible; γ_B is the Blue ground reinforcement rate per fraction of aircraft needed.

2.1.4 | State equations

Mutual attrition and support interactions: Let $I(x > 0) = 1$ if $x > 0$ and 0 otherwise. The following are primitive ordinary stochastic differential equations; see Arnold (1974). For brevity, we only display the state equations for Red variables. The state equations for Blue have the same structure. The change in the number of platforms in each state in a small-time interval dt is the result of independent Poisson random variables which are represented in the model as independent normal random variables with respective means equal to their variances.

$$\begin{aligned}\frac{d}{dt}\boldsymbol{R}_A(t) = &-\underbrace{\beta_B \boldsymbol{B}_A(t) I(\boldsymbol{R}_A(t) > 0)}_{\substack{\text{Attrition of Red aloft a/c}\\ \text{by Blue.Lanchesterian}\\ \text{“aimed fire”}}} + \underbrace{\alpha_R\left[\frac{\overline{R}_A - \boldsymbol{R}_A[t]}{\overline{R}_A}\right]^+ \boldsymbol{R}_G(t)}_{\substack{\text{Re-enforcement}\\ \text{of Red aloft a/c}\\ \text{by Red ground}}}\\ &- \underbrace{\delta_R \boldsymbol{R}_A(t)}_{\substack{\text{Return to base}\\ \text{at end of mission}\\ \text{(endurance)}}} - \sum_c \underbrace{\varphi_{Rc}\boldsymbol{R}_A(t)}_{\substack{\text{Failure type}\\ \text{c of Red aloft}\\ \text{a/c}}}\\ &- \sqrt{\beta_B \boldsymbol{B}_A(t) I(\boldsymbol{R}_A(t) > 0)}\, d\boldsymbol{W}_{RAK}(t)\\ &+ \sqrt{\alpha_R\left[\frac{\overline{R}_A - \boldsymbol{R}_A[t]}{\overline{R}_A}\right]^+ \boldsymbol{R}_G(t)}\, d\boldsymbol{W}_{RAK}(t)\\ &- \sqrt{\delta_R R_A(t)}\, d\boldsymbol{W}_{RE}(t) - \sum_c \sqrt{\varphi_{Rc}\boldsymbol{R}_A(t)}\, d\boldsymbol{W}_{RFc}(t),\end{aligned} \tag{2.1a}$$

$$\begin{aligned}\frac{d}{dt}\boldsymbol{R}_G(t) = &\underbrace{\gamma_R\left[\frac{\overline{R} - \boldsymbol{R}_A(t) - \boldsymbol{R}_G(t) - \sum_c \boldsymbol{R}_c(t)}{\overline{R}}\right]^+}_{\substack{\text{Re-enforcement}\\ \text{of Red a/c on tarmac}\\ \text{by off-site Red}}} + \sum_c \underbrace{\mu_{Rc}\boldsymbol{R}_c(t)}_{\substack{\text{Repair of}\\ \text{Red type c}\\ \text{failure}}}\\ &- \underbrace{\alpha_R\left[\frac{\overline{R}_A - \boldsymbol{R}_A(t)}{\overline{R}_A}\right]^+ \boldsymbol{R}_G(t)}_{\text{Aloft Red reinforcement}} + \underbrace{\delta_R \boldsymbol{R}_A(t)}_{\substack{\text{Aloft}\\ \text{Red mission}\\ \text{duration}\\ \text{ends}}}\\ &+ \sum_c \sqrt{\mu_{Rc}\boldsymbol{R}_c(t)}\, d\boldsymbol{W}_{RRc}(t)\\ &+ \sqrt{\gamma_R\left[\frac{\overline{R} - \boldsymbol{R}_A(t) - \boldsymbol{R}_G(t) - \sum_c \boldsymbol{R}_c(t)}{\overline{R}}\right]^+}\, d\boldsymbol{W}_{RGR}(t)\\ &- \sqrt{\alpha_R \frac{[\overline{R}_A - \boldsymbol{R}_A(t)]^+}{\overline{R}_A} \boldsymbol{R}_G(t)}\, d\boldsymbol{W}_{RAR}(t)\end{aligned}$$

$$+\sqrt{\delta_R \boldsymbol{R}_A(t)}d\boldsymbol{W}_{RE}(t), \tag{2.1b}$$

$$\frac{d}{dt}\boldsymbol{R}_c(t) = -\underbrace{\mu_{Rc}\boldsymbol{R}_c(t)}_{\substack{\text{Repair of}\\ \text{type c}\\ \text{failure}}} + \underbrace{\varphi_{Rc}\boldsymbol{R}_A(t)}_{\substack{\text{Type c}\\ \text{failure}\\ \text{of aloft Red}}} - \sqrt{\mu_{Rc}\boldsymbol{R}_c(t)}d\boldsymbol{W}_{RRc}(t)$$

$$+\sqrt{\varphi_{Rc}\boldsymbol{R}_A(t)}d\boldsymbol{W}_{RFc}(t), \tag{2.1c}$$

$c = 1, 2, \ldots, C$; these are discrete failure mode types.

In all cases, $\boldsymbol{R}_\bullet(t) = [\boldsymbol{R}_\bullet(t)]^+$ and $\boldsymbol{B}_\bullet(t) = [\boldsymbol{B}_\bullet(t)]^+$.

2.2 | A limiting stochastic model for many Blue and Red aircraft

Let n be the sum of the total force size in the theater of Blue and Red, $\overline{R}+\overline{B}$, at time 0. For large n, we consider the state of the system as a deterministic (mean) process plus a diffusion or noise process. To this end, we introduce the standardized noise terms:

$$\boldsymbol{X}_{RA}(t) = \frac{\boldsymbol{R}_A(t) - nr_A(t)}{\sqrt{n}}; \boldsymbol{X}_{RG}(t) = \frac{\boldsymbol{R}_G(t) - nr_G(t)}{\sqrt{n}};$$
$$\boldsymbol{X}_{Rc}(t) = \frac{\boldsymbol{R}_c(t) - nr_c(t)}{\sqrt{n}}$$
$$\boldsymbol{X}_{BA}(t) = \frac{\boldsymbol{B}_A(t) - nb_A(t)}{\sqrt{n}}; \boldsymbol{X}_{BG}(t) = \frac{\boldsymbol{B}_G(t) - nb_G(t)}{\sqrt{n}};$$
$$\boldsymbol{X}_{Bc}(t) = \frac{\boldsymbol{B}_c(t) - nb_c(t)}{\sqrt{n}}, \tag{2.2a}$$

$r_A(t)$, (respectively $b_A(t)$), is the normalized mean number of Red, (respectively Blue), aircraft aloft at time t; $r_G(t)$, (respectively $b_G(t)$) is the normalized mean number of Red (respectively Blue) ready aircraft on the tarmac at time t; $r_c(t)$, (respectively $b_c(t)$), is the normalized mean number of Red (respectively Blue) aircraft being repaired at time t for type c failure.

Equations (2.2a) results in expressions for the state variables:

$$\boldsymbol{R}_A(t) = nr_A(t) + \sqrt{n}\boldsymbol{X}_{RA}(t); \boldsymbol{R}_G(t) = nr_G(t) + \sqrt{n}\boldsymbol{X}_{RG}(t);$$
$$\boldsymbol{R}_c(t) = nr_c(t) + \sqrt{n}\boldsymbol{X}_{Rc}(t); \boldsymbol{B}_A(t) = nb_A(t) + \sqrt{n}\boldsymbol{X}_{BA}(t);$$
$$\boldsymbol{B}_G(t) = nb_G(t) + \sqrt{n}\boldsymbol{X}_{BG}(t); \boldsymbol{B}_c(t) = nb_c(t) + \sqrt{n}\boldsymbol{X}_{Bc}(t). \tag{2.2b}$$

Put $\overline{R}_A = n\overline{R}_A'$, $\overline{B} = n\overline{B}'$, $\overline{B}_A = n\overline{B}_A'$, $\overline{R} = n\overline{R}'$, $\gamma_B = n\gamma_B'$, $\gamma_R = n\gamma_R'$.

Substitute expressions (2.2b) into Equations (2.1a)-(2.1c). For there to be a limiting process as n becomes large, the terms of order n and terms of order $\sqrt{n}$ in the resulting equations must be equal to 0; cf. Gaver and Lehoczky (1976) and McNeil and Schach (1973). The terms of order n result in equations specifying the mean of the limiting process and the terms of order $\sqrt{n}$ result in linear stochastic differential equations for the random terms $\boldsymbol{X}_\bullet(t)$. Details of the resulting stochastic differential equations for Red appear in Appendix A. The equations for Blue have the same structure.

2.3 | Differential equations for the means and covariances of the limiting process

The expected values of the resulting limiting multidimensional process satisfy the system of Equations (A.5a)–(A.7a).

For simplicity, assume there is one type of Blue-failure (respectively Red-failure) and put $\boldsymbol{X}_{Bc}(t) = \boldsymbol{X}_{BC}(t)$ and $\boldsymbol{X}_{Rc}(t) = \boldsymbol{X}_{RC}(t)$. Let $\underline{\boldsymbol{X}}(t) = (\boldsymbol{X}_{RA}(t), \boldsymbol{X}_{RG}(t), \boldsymbol{X}_{RC}(t), \boldsymbol{X}_{BA}(t), \boldsymbol{X}_{BG}(t), \boldsymbol{X}_{BC}(t))^T$ and $\underline{\boldsymbol{W}}(t) = (\underline{\boldsymbol{W}}_R(t), \underline{\boldsymbol{W}}_B(t))^T$ where $\underline{\boldsymbol{W}}_R(t) = (\boldsymbol{W}_{RAK}(t), \boldsymbol{W}_{RAR}(t), \boldsymbol{W}_{RE}(t), \boldsymbol{W}_{RF}(t), \boldsymbol{W}_{RRc}(t)\boldsymbol{W}_{RGR}(t))$ and $\underline{\boldsymbol{W}}_B(t) = (\boldsymbol{W}_{BAK}(t), \boldsymbol{W}_{BAR}(t), \boldsymbol{W}_{BE}(t), \boldsymbol{W}_{BF}(t), \boldsymbol{W}_{BRc}(t), \boldsymbol{W}_{BGR}(t))$.

$\{\boldsymbol{W}_\bullet(t);\ t \geq 0\}$ are independent Weiner processes and v^T denotes the transpose of the row vector v.

Equations (A.5b)–(A.7b) can be written in matrix-vector form as

$$\frac{d}{dt}\underline{\boldsymbol{X}}(t) = \underline{A}\ \underline{\boldsymbol{X}}(t) + \underline{D}\,d\underline{\boldsymbol{W}}(t). \tag{2.3}$$

Let $\underline{C}(t)$ be a matrix whose (i, j)th element is $Cov(\boldsymbol{X}_i(t), \boldsymbol{X}_j(t))$. The variance-covariance matrix of the stochastic process (2.3) satisfies the system of differential equations, cf. Arnold (1974),

$$\frac{d}{dt}\underline{C}(t) = \underline{A}(t)\underline{C}(t) + \underline{C}(t)\underline{A}(t)^T + \underline{D}(t)\underline{D}(t)^T. \tag{2.4}$$

2.4 | The force ratio and loss exchange ratio

The force ratio for aloft aircraft (FOR) at time t is $\frac{\boldsymbol{B}_A(t)}{\boldsymbol{R}_A(t)}$. The loss exchange ratio (LER) at time t is $\frac{\boldsymbol{R}_K(t)}{\boldsymbol{B}_K(t)}$ where $\boldsymbol{B}_K(t)$, (respectively $\boldsymbol{R}_K(t)$), is the number of Blue (respectively Red) aircraft killed during $(0, t]$. Blue has more aloft aircraft (respectively fewer aircraft killed) than Red when the FOR (respectively LER) is greater than 1. A FOR (respectively LER) less than 1 reflects a disadvantage to Blue.

The probability the LER is less than 1 is

$$P\left\{\frac{\boldsymbol{B}_K(t)}{\boldsymbol{R}_K(t)} < 1\right\} = P\{\boldsymbol{B}_K(t) - \boldsymbol{R}_K(t) < 0\}. \tag{2.5}$$

The limiting process, (2.2b), results in $\boldsymbol{B}_K(t) - \boldsymbol{R}_K(t)$ having a normal distribution with mean $E[\boldsymbol{B}_K] - E[\boldsymbol{R}_K]$ and variance $Var[\boldsymbol{B}_K] - 2Cov(\boldsymbol{B}_K, \boldsymbol{R}_K) + Var[\boldsymbol{R}_K]$. If there are no outside reinforcements, $\gamma_R = \gamma_B = 0$, then

$$E[\boldsymbol{R}_K(t)] = \overline{R} - [E[\boldsymbol{R}_A(t)] + E[\boldsymbol{R}_G(t)] + E[\boldsymbol{R}_C(t)]], \tag{2.6a}$$

$$Var[\boldsymbol{R}_K(t)] = Var[\boldsymbol{R}_A(t)] + Var[\boldsymbol{R}_G(t)] + Var[\boldsymbol{R}_C(t)] + 2[Cov(\boldsymbol{R}_A(t), \boldsymbol{R}_G(t)) + Cov(\boldsymbol{R}_A(t), \boldsymbol{R}_C(t)) + Cov(\boldsymbol{R}_G(t), \boldsymbol{R}_C(t))], \tag{2.6b}$$

TABLE 1 Diffusion model and simulation comparison

	Blue failure rate		0.5	0.25	0.025	0.5	0.25	0.025
	Blue repair rate		**0.4**	**0.4**	**0.4**	**0.2**	**0.2**	**0.2**
Number Blue aloft	Mean (Std. dev.)	Simulation	5.25 (2.32)	8.01 (2.80)	15.03 (3.25)	3.45 (1.94)	5.84 (2.53)	14.24 (3.33)
	Mean (Std. dev.)	Diffusion	5.34 (2.31)	8.20 (2.78)	15.13 (3.14)	3.61 (1.91)	6.02 (2.52)	14.43 (3.19)
Number Blue ready	Mean (Std. dev.)	Simulation	3.98 (2.07)	4.01 (2.06)	3.92 (2.06)	2.54 (1.63)	2.75 (1.69)	3.54 (1.97)
	Mean (Std. dev.)	Diffusion	4.05 (2.09)	4.06 (2.10)	3.86 (2.08)	2.63 (1.64)	2.78 (1.72)	3.52 (1.99)
Number Blue in repair	Mean (Std. dev.)	Simulation	6.68 (2.66)	5.18 (2.30)	0.96 (0.96)	9.19 (3.15)	7.73 (2.82)	1.82 (1.33)
	Mean (Std. dev.)	Diffusion	6.86 (2.64)	5.22 (2.26)	0.95 (0.97)	9.59 (3.05)	7.91 (2.81)	1.83 (1.33)
Number Red aloft	Mean (Std. dev.)	Simulation	6.15 (2.51)	4.59 (2.52)	1.87 (1.94)	7.18 (2.48)	5.67 (2.54)	2.08 (2.04)
	Mean (Std. dev.)	Diffusion	6.25 (2.51)	4.70 (2.53)	2.04 (1.69)	7.23 (2.48)	5.75 (2.54)	2.20 (1.81)
Number Red ready	Mean (Std. dev.)	Simulation	1.61 (1.29)	1.24 (1.15)	0.62 (0.83)	1.90 (1.35)	1.49 (1.24)	0.66 (0.86)
	Mean (Std. dev.)	Diffusion	1.62 (1.28)	1.23 (1.14)	0.64 (0.82)	1.89 (1.36)	1.49 (1.24)	0.67 (0.84)
Number Red in repair	Mean (Std. dev.)	Simulation	12.79 (2.86)	10.84 (2.97)	7.09 (2.82)	14.04 (2.85)	12.15 (2.89)	7.30 (2.83)
	Mean (Std. dev.)	Diffusion	12.91 (2.87)	11.00 (2.95)	7.40 (2.76)	14.09 (2.83)	12.24 (2.92)	7.64 (2.82)

$$
\begin{aligned}
Cov(\boldsymbol{B}_K(t), \boldsymbol{R}_K(t)) &= Cov(\boldsymbol{B}_A(t), \boldsymbol{R}_A(t)) \\
&+ Cov(\boldsymbol{B}_A(t), \boldsymbol{R}_G(t)) + Cov(\boldsymbol{B}_A(t), \boldsymbol{R}_C(t)) \\
&+ Cov(\boldsymbol{B}_G(t), \boldsymbol{R}_A(t)) + Cov(\boldsymbol{B}_G(t), \boldsymbol{R}_G(t)) \\
&+ Cov(\boldsymbol{B}_G(t), \boldsymbol{R}_C(t)) + Cov(\boldsymbol{B}_C(t), \boldsymbol{R}_A(t)) \\
&+ Cov(\boldsymbol{B}_C(t), \boldsymbol{R}_G(t)) + Cov(\boldsymbol{B}_C(t), \boldsymbol{R}_C(t)). \qquad (2.6c)
\end{aligned}
$$

The variance of $\boldsymbol{B}_K(t)$ has a similar expression.

3 | COMPARISON OF A CONTINUOUS TIME MARKOV CHAIN MODEL AND THE LIMITING PROCESS

In this section we compare sample means and sample standard deviations of a simulation of a related continuous time Markov chain model with 30 aircraft on each side to the expected values and standard deviations of the limiting process, (2.2b), for the stochastic differential equations (2.1a)–(2.1c). The transition rates of the continuous time Markov chain appear in Appendix B. For all cases in this section $\overline{B} = \overline{B_A} = 30$ and $\overline{R} = \overline{R_A} = 30$; there is one type of failure. The limiting process, (2.2b), uses $n = \overline{R} + \overline{B} = 60$. Further, $\boldsymbol{B}_G(0) = \boldsymbol{R}_G(0) = 30$. The Red attrition parameter against Blue is $\beta_R = 0.03$. The attrition parameter for Blue against Red, $\beta_B = 0.027$. The mean time aloft for both Red and Blue aircraft is $1/\delta_B = 1/\delta_R = 10$ hours; the mean time to turn around a ready aircraft for both Red and Blue, $1/\alpha_B = 1/\alpha_R = 1$ hour; there are no outside reinforcements on either side: $\gamma_B = \gamma_R = 0$; the mean time until failure of Red aircraft, $1/\varphi_R = 100/9$ hours; the mean time for Red aircraft maintenance/repair, $1/\mu_R = 20$ hours. Table 1 displays the expected values and standard deviations of the limiting process compared to the sample means and sample standard deviations of the simulation of the continuous time Markov chain, at $t = 2$ days, (48 hours), for various values of the parameters Blue failure rate, φ_B, and Blue repair rate, μ_B. The simulation has 10,000 independent replications.

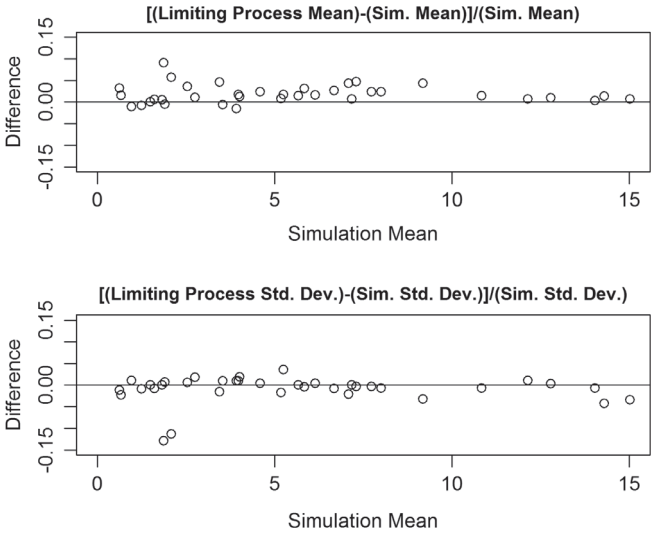

FIGURE 1 Normalized difference between limiting process and simulation results

Figure 1 displays the differences between the limiting process expected value and the simulation sample mean (respectively the limiting process standard deviation minus the simulation sample standard deviation) divided by the simulation sample mean (respectively the simulation sample standard deviation) as a function of the simulation sample mean. The simulation results and the limiting process results for expected value and standard deviation agree reasonably well. Most of the limiting process expected number of aircraft in each state are greater than their corresponding simulation sample mean plus 2 standard errors. However, Figure 1 indicates that the normalized differences between the simulation sample mean and limiting process expected value are less than 10%. The limiting process (2.2b) and the continuous time Markov chain are different. Since the simulation of the continuous time Markov chain has 10,000 replications, it is not surprising that most of limiting process' expected values differ from their corresponding simulation sample means by more than 2 standard errors. A 10% normalized difference

between the two is unlikely to be of operational or managerial significance.

The largest absolute values of the normalized differences for the mean and standard deviation occur when the Blue failure rate is 0.025. In these cases, the mean number of ready Red aircraft on the tarmac is less than 0.7. In all the other cases, the mean number of Red and Blue aircraft in each state is greater than 0.7. The distribution of the limiting process (2.2b) is multivariate normal; if the mean number of aircraft in a state is close to 0, then there can be a substantial positive probability that the number of aircraft in the state is negative. A subject of future study are boundary conditions to ensure that the limiting process values are not negative.

Not surprisingly, the size of the increase in the mean number of Blues aloft when the failure rate φ_B is halved from 0.5 to 0.25 depends on the repair rate μ_B; when the repair rate is 0.4, (respectively 0.2), the mean number of Blues aloft increases by 54% (respectively 74%) when the failure rate decreases from 0.5 to 0.25.

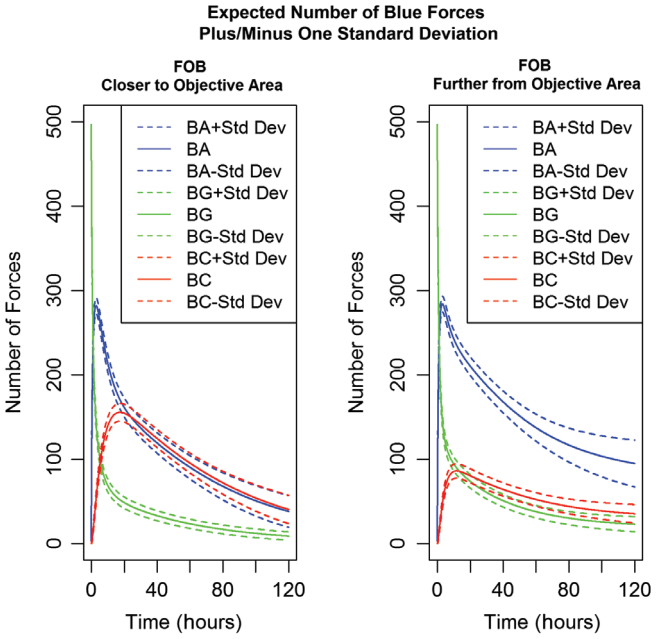

FIGURE 3 Number of Blue forces

4 | EXAMPLE

A medium to large UAV with air-to-air combat capability is expected in approximately 15 years (US Air Force, 2009). We consider a scenario set in the next 15-20 years in which the operational objective is to mass airpower in the form of a swarm of recoverable UAVs with air-to-air combat capability in an objective area to achieve air superiority over Red forces. At this point we assume only unmanned weapon systems on either side, though future work could include a mix of manned and unmanned platforms. A burgeoning literature has emerged that imagines the future of air warfare. For example, Arquilla and Ronfeldt (2000) and Clough (2002) examine UAVs and swarm tactic; while Munoz (2011), Neuenswander (2013), and Sirak (2007) analyze air-to-air warfare specifically.

We consider a simple scenario, displayed in Figure 2, to demonstrate the use of the model. In our scenario, the Blue commander must choose between two forward operating bases (FOBs): LC and LF. The Blue UAVs are repaired and maintained at the FOBs; they fly from the FOB to the objective area to engage aloft Red UAVs. The most obvious difference between the FOBs is their proximity to the objective area. Location LC is closer to the objective area. Location LC allows UAVs more time flying in the objective area.

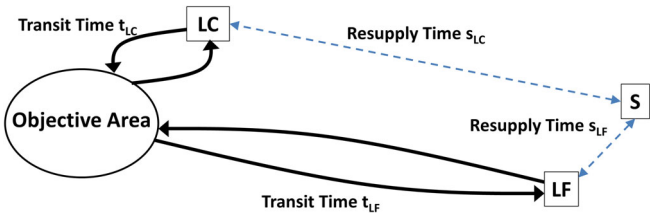

FIGURE 2 Scenario description [Colour figure can be viewed at wileyonlinelibrary.com]

However, it also increases the mean time to repair failures due to increased time to obtain spare parts and subsystems. The characteristics of the scenario primarily impact two parameters in the model. They are β_B, the rate at which a Blue UAV kills Red UAVs and μ_B, the rate at which Blue can respond to maintenance/repair problems.

Both Blue and Red forces have a total of 500 UAVs and observe the battle over the course of 5 days. All aircraft begin in ready status on the tarmac and there is no limit to the proportion of aircraft that either side allows airborne. There is one type of failure. The parameters for Blue aircraft operating from the FOB that is closer to the objective area (LC) and those of Red are: $\overline{B} = \overline{B_A} = 500$ and $\overline{R} = \overline{R_A} = 500$; $\boldsymbol{B}_G(0) = \boldsymbol{R}_G(0) = 500$; $\delta_B = \delta_R = 0.1$; $\varphi_B = \varphi_R = 0.091$; $\alpha_B = \alpha_R = 1$; $\gamma_B = \gamma_R = 0$; $\mu_R = 0.091$; $\beta_R = 0.032$; $\mu_B = 0.1$; $\beta_B = 0.030$. The set of Blue parameters for the FOB that is further away from the objective area (LF) are equal to those of closer location except $\mu_B = 0.25$; $\beta_B = 0.028$.

The limiting process, (2.2b), uses $n = \overline{R} + \overline{B} = 1000$. Figures 3–6 display results for the two possible locations of the FOB. Figure 3, (respectively Figure 4), displays the expected number of Blue, (respectively Red), UAVs in each state plus and minus one standard deviation as a function of time over the course of the 120 hours under consideration. First, we see that when Blue deploys from the closer FOB, the mean number of Blue UAVs aloft (solid blue line) is less than that for the farther location for times greater than 20 hours. The primary difference is that the mean number of Blue UAVs down for maintenance/repair (solid red line) is smaller for the further location due to the higher performance of the logistics system. Comparing the Blue means to the corresponding Red means in Figure 4, we see that the Red and Blue performance is comparable when Blue deploys from the closer location. When Blue deploys from the further location,

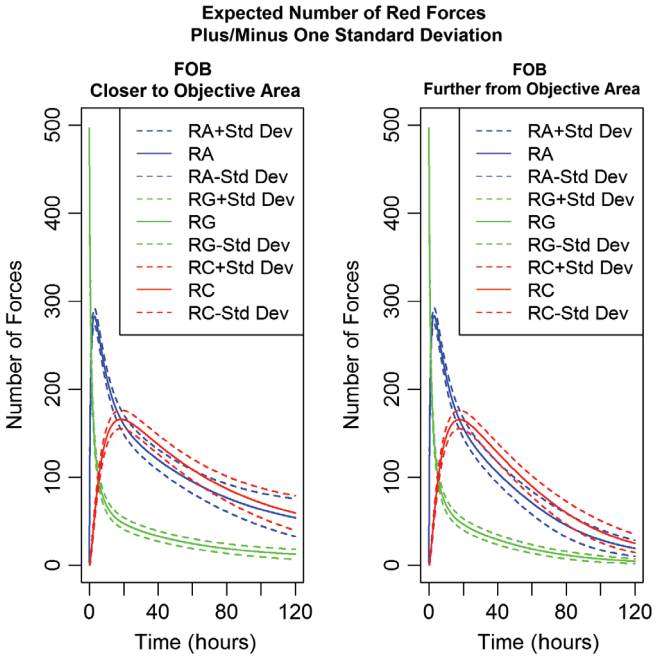

FIGURE 4 Number of Red forces

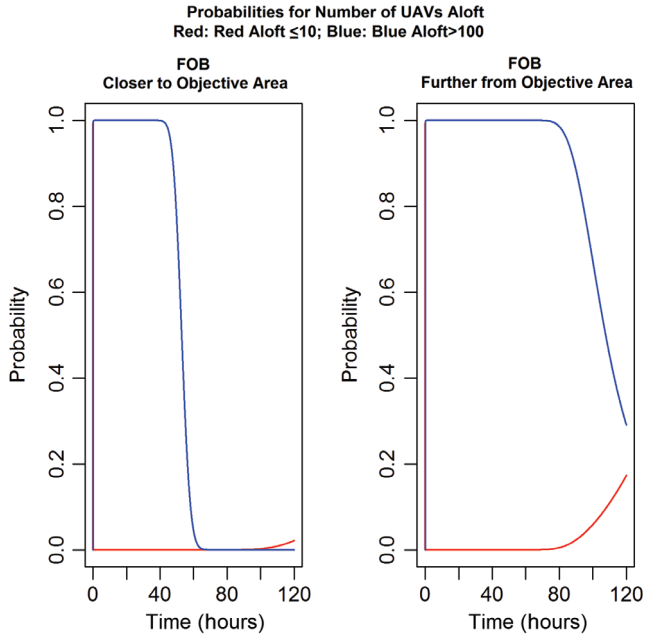

FIGURE 6 Probability for number of UAVs aloft

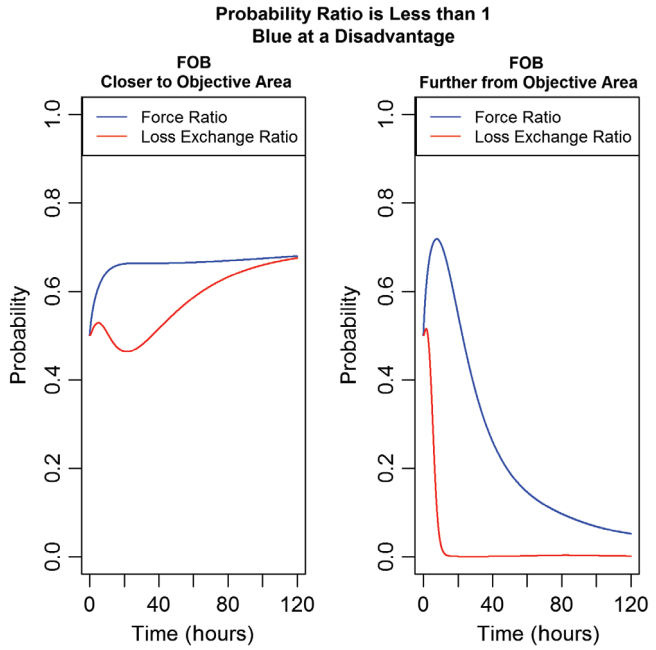

FIGURE 5 Probability ratio is less than 1.0

the mean number of Blue UAVs aloft exceeds that of Red. In this case, the improved logistics system for the more distant Blue location enables Blue to overcome the increased transit time to the objective area, thus offsetting the decrease in the Blue kill rate against Red.

Figure 5 displays the limiting process probability that each of FOR and LER is less than 1 for the two locations. A ratio less than 1 suggests that Blue is at a disadvantage. We define mission success at time 120 hours as having fewer than 10 Red UAVs aloft; having more than 100 Blue UAVs aloft; and having a LER greater than 1. Figure 6 displays the probability that the number of Red UAVs aloft is less than or equal to 10 and the probability the number of Blue UAVs aloft is greater than 100 over the course of 120 hours.

The more distant FOB results in a greater number of Blue UAVs aloft which causes more Red UAVs to be killed compared to that of the FOB closer to the objective area. The FOB further away from the objective area has a smaller probability the LER (respectively FOR) is less than 1 for times greater than 25 hours. The probability that there are more than 100 Blue UAVs aloft for the more distant FOB decreases to less than 0.3 at time 120 hours suggesting risk to mission success.

Next, we vary the Blue failure rate and the number of Blue UAVs to study their impact on operational success. From a programming and budgeting standpoint, decision-makers often must consider where to devote resources to make the most positive impact towards operational success. Our model allows us to quantify the trade-off between improving a design parameter such as the reliability of a system versus simply buying and employing more aircraft. Table 2 displays the mean and standard deviation of the number of Red (respectively Blue) UAVs aloft at time 120 hours; the probability the LER (respectively FOR) is less than 1; and the probability Red (respectively Blue) has fewer than 10 UAVs (respectively more than 100 UAVs) aloft at time 120 hours for the mean Blue repair time, $1/\mu_B = 4$, and various values of the number of Blue UAVs and the Blue failure rate. The other parameters are those of the more distant FOB location.

The first row displays the results from the baseline more distant Blue location, while the next row displays the outcome for Blue UAVs with improved reliability. The third and fourth rows display the results for additional Blue UAVs and the previous failure rates. Decreasing the Blue failure rate from 0.091 to 0.05 has about the same effect as increasing the initial number of Blue UAVs by 50 with the larger Blue failure

TABLE 2 Design parameter trade-offs

Number of Blue UAVs at time 0	Blue failure rate	Number of Red UAVs aloft at $t = 120$ h Mean (standard deviation)	Number of Blue UAVs aloft at $t = 120$ h Mean (standard deviation)	Probability FOR is less than 1 at $t = 120$ h	Probability LER is less than 1 at $t = 120$ h	Probability number of Red UAVs aloft is less than or equal to 10 at $t = 120$ h	Probability number of Blue UAVs aloft is greater than 100 at $t = 120$ h
500	0.091	24.6 (12.4)	82.9 (29.5)	0.03	0.16	0.13	0.03
500	0.05	11.2 (4.5)	138.5(26.0)	0.00	0.00	0.44	1.00
550	0.091	10.6 (3.8)	150.3 (21.3)	0.00	0.00	0.49	1.00
550	0.05	6.6 (2.4)	199.3 (19.5)	0.00	0.00	0.94	1.00

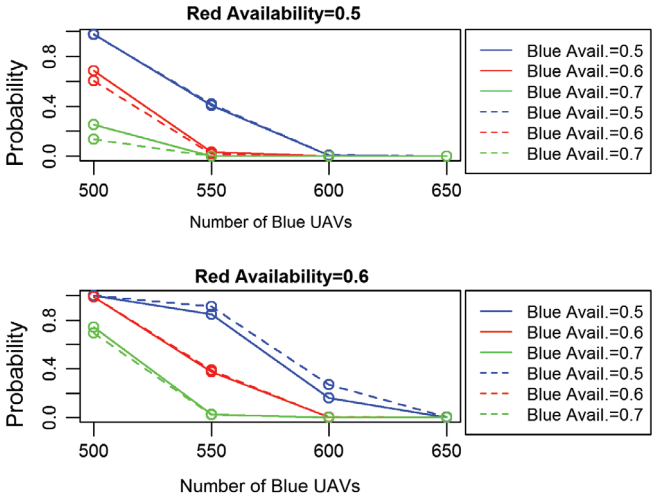

FIGURE 7 Unfavorable LER as a function of number of Blue UAVs and availability

rate 0.091. Not surprisingly, decreasing the Blue failure rate to 0.05 and increasing the number of Blue UAVs to 550 yields the best results.

Finally, we examine the effect of the availability of the aircraft. The long run average proportion of time a Blue UAV is up, ignoring turnaround time, is $\frac{1/\varphi_B}{(1/\varphi_B)+(1/\mu_B)}$, which we call the availability of the Blue UAV; the availability of the Red UAV is defined similarly. Figure 7 displays the probability the LER is less than 1 (Blue is at a disadvantage) at time 120 hours for Red UAV availability equal to 0.5 and 0.6 for various values of Blue UAV availability and various values of the number of Blue UAVs at time 0; all Red and Blue UAVs are ready on the tarmac at time 0; the Red and Blue UAV failure rates are equal. The parameters for Figure 7 are those of the closer FOB except for the Blue aimed fire attrition rate against Red whose value is that of the more distant FOB giving each Blue UAV a disadvantage:

$$R(0) = \overline{R} = \overline{R_A} = 500; \quad \delta_R = \delta_B = 0.1; \quad \alpha_R = \alpha_B = 1;$$
$$\beta_R = 0.032; \quad \beta_B = 0.025.$$

The solid (respectively dashed) line in Figure 7 corresponds to the common Red and Blue failure rate equal to 0.05 (respectively 0.091).

Figure 7 suggests that the probability is a nonlinear function of the Red and Blue failure rates and availabilities. When Red availability is 0.6 and Blue availability is 0.5, the probability associated with the common failure rate of 0.091 is greater than that associated with the common failure rate of 0.5. In the other cases Blue availability is greater than or equal to Red availability and the probability associated with the common failure rate of 0.091 is about equal to or less than the probability associated with the common failure rate of 0.05. In these cases, a common failure rate equal to 0.05 results in more Blue UAVs being airborne causing a greater Blue exposure to Red attrition than the common failure rate 0.091. Not surprisingly, the probability decreases as the Blue availability increases and as the number of Blue UAVs increases. The probability values associated with Red availability equal to 0.6 are greater than or equal to those associated with Red availability equal to 0.5.

5 | DISCUSSION

Deploying manned and unmanned aircraft that succeed in combat in the future will require a robust and responsive logistics system to ensure a high state of operational readiness. A parsimonious diffusion model of the effect of logistics on an aerial battle between Red and Blue forces has been presented. A limiting process for many aircraft on both sides is obtained. Results from the limiting process compare favorably to those from a simulation of a related continuous time Markov chain. The limiting process allows assessment of uncertainty in measures of performance such as force ratio and loss exchange ratio giving more information to the decision maker concerning mission risk. Numerical examples illustrate the model's use in making operational decisions regarding dispositions of forces, as well as exploration of design trade-offs.

ACKNOWLEDGMENTS

The authors thank Jeffrey Kline and Connor McLemore for helpful comments on earlier versions of the manuscript, as well as two anonymous reviewers and the associate editor for their contributions to improving the final version. The views and opinions expressed in this article are those of the authors and do not necessarily reflect the official policy or position of any agency of the U.S. Government.

ORCID

Chad W. Seagren https://orcid.org/0000-0003-2854-9006

REFERENCES

Ancker, C. J. (1967). The status of developments in the theory of stochastic duels – II. *Operations Research*, *15*(3), 388–406.

Arnold, L. (1974). Stochastic differential equations: Theory and applications. New York, NY: John Wiley and Sons.

Arquilla, J., & Ronfeldt, D. (2000). *Swarming and the future of conflict*. RAND technical report D8-311-OSD, Santa Monica, CA.

Artelli, M. J., & Deckro, R. F. (2008). Modeling the Lanchester laws with system dynamics. *The Journal of Defense Modeling and Simulation: Applications, Methodology, Technology*, *5*(1), 1–20.

Balogh, I., & Harless, G. (2003). *An overview of the COMBAT XXI simulation model: A model for the analysis of land and amphibious warfare*. In Proceedings of 71st military operations research society symposium. USMCB: Quantico, VA.

Bazin de Jessey, L., & Debache, G. (2002). *Simulation of aircraft deployment support*. Defense Technical Information Center, Accession Number ADP014149.

Beamon, B. (1998). Supply chain design and analysis: Models and methods. *International Journal of Production Economics*, *55*(3), 281–294.

Bonder, S. (1967). The Lanchester attrition-rate coefficient. *Operations Research*, *15*(2), 221–232.

Bracken, J. (1995). Lanchester models of the Ardennes campaign. *Naval Research Logistics*, *42*(4), 559–577.

Bracken, J., Kress, M., & Rosenthal, R. (Eds.). (1995). Warfare modeling. New York, NY: John Wiley.

Brackney, J. (1959). The dynamics of military combat. *Operations Research*, *7*(1), 30–44.

Chase, M. W. (1973). A *Lanchester-type model with logistics considerations* (MS thesis in Operations Research). Naval Postgraduate School, Monterey, CA.

Clough, B. T. (2002). *UAV swarming? So what are those swarms, what are the implications, and how do we handle them?* Air Force Research Laboratory Air Vehicles Directorate technical report AFRL-VA-WP-TP-2002-308, Dayton, OH.

Deitchman, S. J. (1962). A Lanchester model of guerrilla warfare. *Operations Research*, *10*(6), 818–827.

Gaver, D. P., Isaacson, K. E., & Abell, J. (1993). *Estimating aircraft recoverable spares requirements with cannibalization of designated items*. RAND report R-4213-AF, Santa Monica CA.

Gaver, D. P., & Lehoczky, J. P. (1976). Gaussian approximations to service problems: A communication system example. *Journal of Applied Probability*, *13*, 768–780.

Gilbert, R. E. (2011). *Strategic implications of U.S. fighter force reductions: Air-to-air combat modeling using Lanchester equations*. Graduate Research Paper, Air Force Institute of Technology.

Gue, K. R. (2003). A dynamic distribution model for combat logistics. *Computers and Operations Research*, *30*(3), 367–381.

Hoover, J., Jondrow, J., Trost, R., & Ye, M. (2002). *A model to study: Cannibalization, FMC, and customer waiting time*. Center for Naval Analyses Research Memorandum D0005957.A2/Final.

Huffaker, J.W. (1996). *Modeling the effects of logistics on ground combat and maneuver* (MS thesis in Operations Research). Naval Postgraduate School, Monterey, CA.

Hughes, W. P., Jr. (1995). A salvo model of warships in missile combat used to evaluate their staying power. *Naval Research Logistics*, *42*(2), 267–289.

Johnson, I. R., & MacKay, N. J. (2011). Lanchester models and the Battle of Britain. *Naval Research Logistics*, *58*, 210–222.

Kang, K., Doerr, K., & Sanchez, S. (2006). *A design of experiments approach to readiness risk analysis*. In L. F. Perrone, F. P. Wieland, J. Liu, B. G. Lawson, M. Nicol, & R. M. Fujimoto (Eds.), Proceedings of the 2006 winter simulation conference.

Kang, K., Gue, K., & Eaton, D. (1998). *Cycle time reduction for naval aviation depots*. In D. J. Medeiros, E. F. Watson, J. S. Carson, & M. S. Manivannan (Eds.), Proceedings of the 1998 winter simulation conference.

Kang, K., & McDonald, M. (2010). *Impact of logistics on readiness and life cycle cost: A design of experiments approach*. In B. Johansson, S. Jain, J. Montoya-Torres, J. Hugan, & E. Yucesan (Eds.), Proceedings of the 2010 winter simulation conference.

Karr, A. F. (1974). *Stochastic attrition models of Lanchester type*. Institute for Defense Analysis Paper P-1030.

Kress, M., & Talmor, I. (1999). A new look at the 3:1 rule of combat through Markov stochastic Lanchester models. *Journal of the Operational Research Society*, *50*(7), 733–744.

Lanchester, F. W. (1916). Aircraft in warfare: The Dawn of the fourth arm. London, England: Constable and Company Limited.

Lucas, T. W., & Turkes, T. (2004). Fitting Lanchester equations to the battles of Kursk and Ardennes. *Naval Research Logistics*, *51*(1), 95–116.

McGlynn, T. P. (2000). Do Lanchester's laws of combat describe competition in ants? *Behavioral Ecology*, *11*(6), 686–690.

McLemore, C., Gaver, D. P., & Jacobs, P. A. (2016). A model for geographically distributed combat interactions of swarming naval and air forces. *Naval Research Logistics*, *63*(7), 562–576.

McNeil, D. R., & Schach, S. (1973). Central limit theorem analogues for Markov population processes. *Journal of Royal Statistical Society. Series B*, *35*, 1–23.

Moglewer, S., & Payne, C. (1970). A game theory approach to logistics allocation. *Naval Research Logistics*, *17*(1), 87–97.

Munoz, M. F. (2011). *Agent-based simulation and analysis of a defensive UAV swarm against and enemy UAV swarm* (PhD thesis). Naval Postgraduate School, Monterey, CA.

Neuenswander, D. M., (2013). *Wargaming the enemy unmanned aircraft system (UAS) threat*. Army Training and Doctrine Command technical report, Fort Leavenworth, KS.

Øksendal, B. (2013). Stochastic differential equations: An introduction with applications (6th ed., 6th corrected printing). New York, NY: Springer.

Perlas, P. P., & Lehoczky, J. P. (1977). *A new approach to the analysis of stochastic Lanchester processes. I. Time evolution*. Technical Report, Statistics Department, Carnegie Mellon University.

Saie, C. M., & Ahner, D. K. (2018). Investigating the dynamics of nation-building through a system of differential equations. *Journal of Operational Research Society*, *69*(4), 619–629.

Schaffer, M. B. (1968). Lanchester models of guerrilla engagements. *Operations Research*, *16*(3), 457–488.

Schramm, H. C., & Gaver, D. P. (2013). Lanchester for cyber: The mixed epidemic-combat model. *Naval Research Logistics*, *60*(7), 599–605.

Sirak, M. (2007). Atk unveils counter uav systems as part of growing portfolio. *Defense Daily*, *235*(36), 2–3.

Sullivan, J., Crone, L., & Jalickee, J. (1980). Approximation of the unit step function by a linear combination of exponential functions. *Journal of Approximation Theory*, *28*, 299–308.

Taylor, J. G. (1983). Lanchester models of warfare. *Operations Research Society of America*, *I and II*.

US Air Force. (2009). Unmanned aircraft systems flight plan 2009–2047. Washington, DC: Headquarters Department of the Air Force.

Washburn, A., & Kress, M. (2009). Combat modeling. New York, NY: Springer.

Weiss, H. K. (1966). Combat models and historical data: The U.S. civil war. *Operations Research*, *14*(5), 759–790.

Wilson, M. L., Britton, N. F., & Franks, N. R. (2002). Chimpanzees and the mathematics of battle. *Proceedings of the Royal Society of Biological Sciences*, *269*(1496), 1107–1112.

Yavuz, I., & Satir, A. (1995). Kanban-based operational planning and control: Simulation modeling. *Production Planning and Control*, *6*(4), 331–344.

How to cite this article: Seagren CW, Gaver DP, Jacobs PA. A stochastic air combat logistics decision model for Blue versus Red opposition. *Naval Research Logistics* 2019;66:663–674. https://doi.org/10.1002/nav.21876

APPENDIX A: THE LIMITING STOCHASTIC MODEL

We approximate the nonlinear function $[x]^+$ appearing in Equations (2.1a)-(2.1c) with a linear function by invoking the first two terms of its Taylor series expansion.

$$\left[\frac{\overline{R}_A' - \left[r_A(t) + \frac{1}{\sqrt{n}}\boldsymbol{X}_{RA}(t)\right]}{\overline{R}_A'}\right]^+ = \left[\frac{\overline{R}_A' - r_A(t)}{\overline{R}_A'}\right]^+ - I(\overline{R}_A' - r_A(t) > 0)\frac{1}{\overline{R}_A'}\frac{1}{\sqrt{n}}\boldsymbol{X}_{RA}(t). \quad \text{(A.1)}$$

The gamma cumulative distribution function is a common smooth approximation for the indicator function $I(x > 0)$; in particular we use the *gamma cumulative distribution* function with shape parameter = 2 and mean = 0.03 as a smooth approximation to $I(x > 0)$; other approximations are possible, cf. Sullivan, Crone, and Jalickee (1980). Specifically, for $x > 0$

$$I(x > 0) \approx f_I(x) = 1 - \exp\left\{-\frac{200}{3}x\right\} - \frac{200}{3}x\exp\left\{-\frac{200}{3}x\right\} \quad \text{(A.2)}$$

with derivative

$$f_I'(x) = \left(\frac{200}{3}\right)^2 x\exp\left\{-\frac{200}{3}x\right\}. \quad \text{(A.3)}$$

Thus

$$I\left(r_A(t) + \frac{1}{\sqrt{n}}\boldsymbol{X}_{RA}(t) > 0\right) \approx f_I(r_A(t)) + f_I'(r_A(t))\frac{1}{\sqrt{n}}\boldsymbol{X}_{RA}(t). \quad \text{(A.4)}$$

Inserting (2.2b) into (2.1a) and using approximations similar to (A.1) and (A.4) results in

$$\frac{d}{dt}[nr_A(t) + \sqrt{n}\boldsymbol{X}_{RA}(t)] = \underbrace{-\beta_B[nb_A(t) + \sqrt{n}\boldsymbol{X}_{BA}(t)]\times\left[f_I(r_A(t)) + f_I'(r_A(t))\frac{1}{\sqrt{n}}\boldsymbol{X}_{RA}(t)\right]}_{\text{Attrition of Red aloft a/c by Blue.Lanchesterian “aimed fire”}}$$

$$+ \underbrace{\alpha_R\left[\left[\frac{\overline{R}_A' - r_A(t)}{\overline{R}_A'}\right]^+ - I\left(\overline{R}_A' - r_A(t) > 0\right)\frac{1}{\sqrt{n}}\frac{1}{\overline{R}_A'}\boldsymbol{X}_{RA}(t)\right]\times[nr_G(t) + \sqrt{n}\boldsymbol{X}_{RG}(t)]}_{\text{Re-enforcement of Red aloft a/c by Red ground}}$$

$$- \underbrace{\delta_R[nr_A(t) + \sqrt{n}\boldsymbol{X}_{RA}(t)]}_{\text{Return to base at end of mission (endurance)}} - \underbrace{\varphi_R[nr_A(t) + \sqrt{n}\boldsymbol{X}_{RA}(t)]}_{\text{Return to base due to failure (unreliable)}}$$

$$- \sqrt{\beta_B[nb_A(t) + \sqrt{n}\boldsymbol{X}_{BA}(t)]\times\left[f_I(r_A(t)) + f_I'(r_A(t))\frac{1}{\sqrt{n}}\boldsymbol{X}_{RA}(t)\right]}\,d\boldsymbol{W}_{RAK}(t)$$

$$+ \sqrt{\alpha_R\left[\left[\left[\frac{\overline{R}_A' - r_A(t)}{\overline{R}_A'}\right]^+ - I\left(\overline{R}_A' - r_A(t) > 0\right)\times\frac{1}{\sqrt{n}}\frac{1}{\overline{R}_A'}\boldsymbol{X}_{RA}(t)\right]\right]\times[nr_G(t) + \sqrt{n}\boldsymbol{X}_G(t)]}\,d\boldsymbol{W}_{RAR}[t]$$

$$- \sqrt{\delta_R[nr_A(t) + \sqrt{n}\boldsymbol{X}_{RA}(t)]}\,d\boldsymbol{W}_{RE}(t)$$

$$- \sqrt{\varphi_R[nr_A(t) + \sqrt{n}\boldsymbol{X}_{RA}(t)]}\,d\boldsymbol{W}_{RF}(t).$$

Identify terms of order n:

$$\frac{d}{dt}r_A(t) = -\beta_B b_A(t)f_I(r_A(t)) + \alpha_R\left[\frac{\overline{R}_A' - r_A[t]}{\overline{R}_A'}\right]^+ \times r_G(t) - \delta_R r_A(t) - \varphi_R r_A(t). \quad \text{(A.5a)}$$

Identify terms of order $\sqrt{n}$:

$$\begin{aligned}\frac{d}{dt}\boldsymbol{X}_{RA}(t) =& -\beta_B I(b_A(t) > 0)f_I(r_A(t))I(r_A(t) > 0)\boldsymbol{X}_{BA}(t)\\ &- \beta_B b_A(t)f_I'(r_A(t))I(r_A(t) > 0)\boldsymbol{X}_{RA}(t)\\ &+ \alpha_R\left[\frac{\overline{R}_A' - r_A(t)}{\overline{R}_A'}\right]^+ I(r_G(t) > 0)\boldsymbol{X}_{RG}(t)\\ &- \alpha_R I(\overline{R}_A' - r_A(t) > 0)r_G(t)\frac{1}{\overline{R}_A'}\boldsymbol{X}_{RA}(t)\\ &- [\delta_R + \varphi_R]I(r_A(t) > 0)\boldsymbol{X}_{RA}(t)\\ &- \sqrt{\beta_B f_I(r_A(t))b_A(t)I(r_A(t) > 0)}\,d\boldsymbol{W}_{RAK}(t)\\ &+ \sqrt{\alpha_R\left[\frac{\overline{R}_A' - r_A(t)}{\overline{R}_A'}\right]^+ r_G(t)}\,d\boldsymbol{W}_{RAR}(t)\\ &- \sqrt{\delta_R r_A(t)}\,d\boldsymbol{W}_{RE}(t) - \sqrt{\varphi_R r_A(t)}\,d\boldsymbol{W}_{RF}(t).\end{aligned} \quad \text{(A.5b)}$$

Insert (2.2b) into (2.1b) and using approximations similar to (A.1) and (A.4).

Identify terms of order n:

$$\frac{d}{dt}r_G(t) = \gamma_R\left[\frac{\overline{R}' - r_A(t) - r_G(t) - \sum_c r_c(t)}{\overline{R}\prime}\right]^+ - \alpha_R\left[\frac{\overline{R}_A' - r_A(t)}{\overline{R}_A'}\right]^+ r_G(t) + \delta_R r_A(t) + \sum_c \mu_{Rc}r_c(t). \quad \text{(A.6a)}$$

Identify terms of order $\sqrt{n}$:

$$\begin{aligned}
\frac{d}{dt}\boldsymbol{X}_{RG}(t) &= -\alpha_R\left[\frac{\overline{R}_A' - r_A(t)}{\overline{R}_A'}\right]^+ I(r_G(t)>0)\boldsymbol{X}_{RG}(t)\\
&+ \alpha_R I(\overline{R}_A' - r_A(t)>0) r_G(t)\frac{1}{\overline{R}_A'} I(r_A(t)>0)\boldsymbol{X}_{RA}(t)\\
&- \gamma_R' I\left(\overline{R}' - r_A(t) - r_G(t) - \sum_c r_c(t) > 0\right)\\
&\times \frac{1}{\overline{R}'}\left[\boldsymbol{X}_{RA}(t) + \boldsymbol{X}_{RG}(t) + \sum_c \boldsymbol{X}_{RRc}(t)\right]\\
&+ \delta_R I(r_A(t)>0)\boldsymbol{X}_{RA}(t)\\
&+ \sum_c \mu_{Rc} I(r_c(t)>0)\boldsymbol{X}_{RRc}(t)\\
&- \sqrt{\alpha_R\left[\frac{\overline{R}_A' - r_A(t)}{\overline{R}_A'}\right]^+ r_G(t)}\,d\boldsymbol{W}_{RAR}(t)\\
&+ \sum_c \sqrt{\mu_{Rc} r_c(t)}\,d\boldsymbol{W}_{RRc}(t)\\
&+ \sqrt{\gamma_R'\left[\frac{\overline{R}' - r_A(t) - r_G(t) - \sum_c r_c(t)}{\overline{R}'}\right]^+}\,d\boldsymbol{W}_{RGR}(t)\\
&+ \sqrt{\delta_R r_A(t)}\,d\boldsymbol{W}_{RE}(t). \qquad \text{(A.6b)}
\end{aligned}$$

Insert (2.2b) into (2.1c) and using approximations similar to (A.1) and (A.4).

Identify terms of order n:

$$\frac{d}{dt}r_c(t) = -\mu_{Rc} r_c(t) + \varphi_{Rc} r_A(t) \qquad \text{(A.7a)}$$

Identify terms of order $\sqrt{n}$:

$$\begin{aligned}
\frac{d}{dt}\boldsymbol{X}_{Rc}(t) &= -\mu_{Rc} I(r_c(t)>0)\boldsymbol{X}_{Rc}(t) + \varphi_{Rc} I(r_A(t)>0)\boldsymbol{X}_{RA}(t)\\
&- \sqrt{\mu_{Rc} r_c(t)}\,d\boldsymbol{W}_{RRc}(t) + \sqrt{\varphi_{Rc} r_A(t)}\,d\boldsymbol{W}_{RFc}(t). \qquad \text{(A.7b)}
\end{aligned}$$

APPENDIX B: THE TRANSITION RATES OF THE CONTINUOUS TIME MARKOV CHAIN MODEL

Let

$$\begin{aligned}
\underline{\boldsymbol{Y}}(t) = (\underline{\boldsymbol{R}}(t), \underline{\boldsymbol{B}}(t)) = (&\boldsymbol{R}_A(t), \boldsymbol{R}_G(t),\\
&\boldsymbol{R}_C(t), \boldsymbol{B}_A(t), \boldsymbol{B}_G(t), \boldsymbol{B}_C(t)). \qquad \text{(B.1)}
\end{aligned}$$

The means and variances of the limiting process (2.2b) are compared to that of a simulation of a continuous time Markov chain model with transition rates

$$\begin{aligned}
P\{\underline{\boldsymbol{Y}}(t+h) &= (r_A - 1, r_G, r_C, b_A, b_G, b_C) | \underline{\boldsymbol{Y}}(t)\\
&= (r_A, r_G, r_C, b_A, b_G, b_C)\}\\
&= \beta_B b_A I(r_A>0)h + o(h), \qquad \text{(B.2a)}
\end{aligned}$$

$$\begin{aligned}
P\{\underline{\boldsymbol{Y}}(t+h) &= (r_A + 1, r_G - 1, r_C, b_A, b_G, b_C) | \underline{\boldsymbol{Y}}(t)\\
&= (r_A, r_G, r_C, b_A, b_G, b_C)\}\\
&= \alpha_R\left[\frac{\overline{R}_A - r_A}{\overline{R}_A}\right]^+ r_G h + o(h), \qquad \text{(B.2b)}
\end{aligned}$$

$$\begin{aligned}
P\{\underline{\boldsymbol{Y}}(t+h) &= (r_A - 1, r_G + 1, r_C, b_A, b_G, b_C) | \underline{\boldsymbol{Y}}(t)\\
&= (r_A, r_G, r_C, b_A, b_G, b_C)\} = \delta_R r_A h + o(h), \qquad \text{(B.2c)}
\end{aligned}$$

$$\begin{aligned}
P\{\underline{\boldsymbol{Y}}(t+h) &= (r_A - 1, r_G, r_C + 1, b_A, b_G, b_C) | \underline{\boldsymbol{Y}}(t)\\
&= (r_A, r_G, r_C, b_A, b_G, b_C)\}\\
&= \varphi_R r_A h + o(h), \qquad \text{(B.2d)}
\end{aligned}$$

$$\begin{aligned}
P\{\underline{\boldsymbol{Y}}(t+h) &= (r_A, r_G + 1, r_C - 1, b_A, b_G, b_C) | \underline{\boldsymbol{Y}}(t)\\
&= (r_A, r_G, r_C, b_A, b_G, b_C)\}\\
&= \mu_R r_C h + o(h), \qquad \text{(B.2e)}
\end{aligned}$$

$$\begin{aligned}
P\{\underline{\boldsymbol{Y}}(t+h) &= (r_A, r_G + 1, r_C, b_A, b_G, b_C) | \underline{\boldsymbol{Y}}(t)\\
&= (r_A, r_G, r_C, b_A, b_G, b_C)\}\\
&= \gamma_R\left[\frac{\overline{R} - r_A - r_G - r_C}{\overline{R}}\right]^+ h + o(h). \qquad \text{(B.2f)}
\end{aligned}$$

$$\begin{aligned}
P\{\underline{\boldsymbol{Y}}(t+h) &= (r_A, r_G, r_C, b_A - 1, b_G, b_C) | \underline{\boldsymbol{Y}}(t)\\
&= (r_A, r_G, r_C, b_A, b_G, b_C)\}\\
&= \beta_R r_A I(b_A>0)h + o(h), \qquad \text{(B.3a)}
\end{aligned}$$

$$\begin{aligned}
P\{\underline{\boldsymbol{Y}}(t+h) &= (r_A, r_G, r_C, b_A + 1, b_G - 1, b_C) | \underline{\boldsymbol{Y}}(t)\\
&= (r_A, r_G, r_C, b_A, b_G, b_C)\}\\
&= \alpha_B\left[\frac{\overline{B}_A - b_A}{\overline{B}_A}\right]^+ b_G h + o(h), \qquad \text{(B.3b)}
\end{aligned}$$

$$\begin{aligned}
P\{\underline{\boldsymbol{Y}}(t+h) &= (r_A, r_G, r_C, b_A - 1, b_G + 1, b_C) | \underline{\boldsymbol{Y}}(t)\\
&= (r_A, r_G, r_C, b_A, b_G, b_C)\}\\
&= \delta_B b_A h + o(h), \qquad \text{(B.3c)}
\end{aligned}$$

$$\begin{aligned}
P\{\underline{\boldsymbol{Y}}(t+h) &= (r_A, r_G, r_C, b_A - 1, b_G, b_C + 1) | \underline{\boldsymbol{Y}}(t)\\
&= (r_A, r_G, r_C, b_A, b_G, b_C)\}\\
&= \varphi_B b_A h + o(h), \qquad \text{(B.3d)}
\end{aligned}$$

$$\begin{aligned}
P\{\underline{\boldsymbol{Y}}(t+h) &= (r_A, r_G, r_C, b_A, b_G + 1, b_C - 1) | \underline{\boldsymbol{Y}}(t)\\
&= (r_A, r_G, r_C, b_A, b_G, b_C)\}\\
&= \mu_B b_C h + o(h), \qquad \text{(B.3e)}
\end{aligned}$$

$$\begin{aligned}
P\{\underline{\boldsymbol{Y}}(t+h) &= (r_A, r_G, r_C, b_A, b_G + 1, b_C) | \underline{\boldsymbol{Y}}(t)\\
&= (r_A, r_G, r_C, b_A, b_G, b_C)\}\\
&= \gamma_B\left[\frac{\overline{B} - b_A - b_G - b_C}{\overline{B}}\right]^+ h + o(h). \qquad \text{(B.3f)}
\end{aligned}$$